

Towards Pure End-to-End Learning for Recognizing Multiple Text Sequences from an Image

Zhenlong Xu^{1*}

Fan Bai¹

Shuigeng Zhou^{1†}

Yi Niu²

Zhanzhan Cheng²

Shiliang Pu²

¹Shanghai Key Lab of Intelligent Information Processing, and School of
Computer Science, Fudan University, Shanghai 200433, China

²Hikvision Research Institute, China

{zlxu18, sgzhou, fbai17}@fudan.edu.cn

{chengzhanzhan, niuyi, pushiliang}@hikvision.com

Abstract

Here we address a challenging problem: recognizing multiple text sequences from an image by pure end-to-end learning. It is twofold: 1) Multiple text sequences recognition. Each image may contain multiple text sequences of different content, location and orientation, and we try to recognize all the text sequences contained in the image. 2) Pure end-to-end (PEE) learning. We solve the problem in a pure end-to-end learning way where each training image is labeled by only text transcripts of all contained sequences, without any geometric annotations.

Most existing works recognize multiple text sequences from an image in a non-end-to-end (NEE) or quasi-end-to-end (QEE) way, in which each image is trained with both text transcripts and text locations. Only recently, a PEE method was proposed to recognize text sequences from an image where the text sequence was split to several lines in the image. However, it cannot be directly applied to recognizing multiple text sequences from an image.

So in this paper, we propose a pure end-to-end learning method to recognize multiple text sequences from an image. Our method directly learns multiple sequences of probability distribution conditioned on each input image, and outputs multiple text transcripts with a well-designed decoding strategy. To evaluate the proposed method, we constructed several datasets mainly based on an existing public dataset and two real application scenarios. Experimental results show that the proposed method can effectively recognize multiple text sequences from images, and outperforms CTC-based and attention-based baseline methods.

1. Introduction

Recognizing text from images, evolved from the classical optical character recognition (OCR) problem, has been a popular research topic [6, 12, 28, 30] in pattern recognition and computer vision areas for more than a decade, due to its wide applications such as handwriting recognition, automatic card reading, and image understanding. Though significant technical progress has been made, this problem is far from being well solved, considering various complex application scenarios.

Existing works [18, 19, 33, 34] of text recognition from images mainly employ a pipeline that contains a text detection module and a text recognition module. The former is used to detect text content (e.g. characters, words or text sequences) in images, while the latter is responsible for reading the cropped text images. Technically, we can subsume these works into *non-end-to-end* (NEE for short) methods. However, given an image containing multiple text sequences, these methods have to first detect these sequences, and then recognize them one by one.

With the popularity of deep learning, more and more works [10, 17, 21] attempt to read text in an “end-to-end” way by first pre-training the detection module or recognition module, and then conducting a joint training on the detection and recognition tasks. Different from the early NEE methods, they integrate the detection module and recognition module into a unified network, but still train the whole model with both text transcripts and geometric annotations (e.g. bounding boxes). Therefore, we call them *quasi-end-to-end* (QEE) methods.

Recently, Bluche *et al.* [4] proposed an attention based method to recognize text lines from images in a *pure end-to-end* (PEE for short) way. We say it is a PEE method in the sense that the training images are annotated with *only* text content, no location information is needed. However,

*Zhenlong Xu did most of this work when he was an intern in Hikvision Research Institute.

†Corresponding author.

this method can recognize only one text sequence from an image. Though the target text sequence may split into several lines in the image, they treat the text lines as a whole, and the order of text lines constituting the sequence must be pre-defined. Essentially, this method can handle only *single sequence recognition* (SSR) problem.

In this paper, we try to tackle a new and more challenging problem: recognizing multiple text sequences from an image by pure end-to-end learning. This problem is twofold: 1) *Multiple text sequence recognition*. Each image may contain multiple *independent* text sequences with different layouts, and we try to recognize all these text sequences. In one word, our problem is a *multiple-sequence recognition* (MSR) problem. We show some MSR examples in Fig. 1. 2) *Pure end-to-end (PEE) learning*. Each training image is annotated with *only* text transcripts. Our goal is to solve the MSR problem with a PEE method.

Generally, existing NEE and QEE methods cannot handle our problem, because they are not PEE methods. The method of Bluche *et al.* [4] can neither. Though it is a PEE method, it is for the SSR problem, at least cannot be straightforwardly applied to our problem. Therefore, we have to explore new method. For better understanding the problem we try to address and the differences between our work and the existing works, we compare NEE, QEE and PEE in Tab. 1, and highlight the differences between our work and the typical existing works in Tab. 2.

Table 1: Comparison of NEE, QEE and PEE. ‘T’ means text transcripts and ‘G’ means geometric annotations; ‘D’ means detector and ‘R’ means recognizer.

| Method | Architecture | Annotations |
|--------|--------------|-------------|
| NEE | Separate D/R | T+G |
| QEE | Joint D-R | T+G |
| PEE | R | T |

Table 2: A comparison of our work with typical existing works from two perspectives: *addressed problem* (MSR or SSR) and *employed method* (NEE, QEE or PEE).

| Problem | Method | Typical works |
|---------|--------|------------------|
| MSR | NEE | [18, 19, 33, 34] |
| MSR | QEE | [10, 17, 21, 23] |
| SSR | PEE | [4] |
| MSR | PEE | Ours |

To solve this problem, we first consider the connectionist temporal classification [8] (CTC) mechanism and the *attention* mechanism [1]. Both of them are popular in SSR but cannot directly read images with multiple text sequences

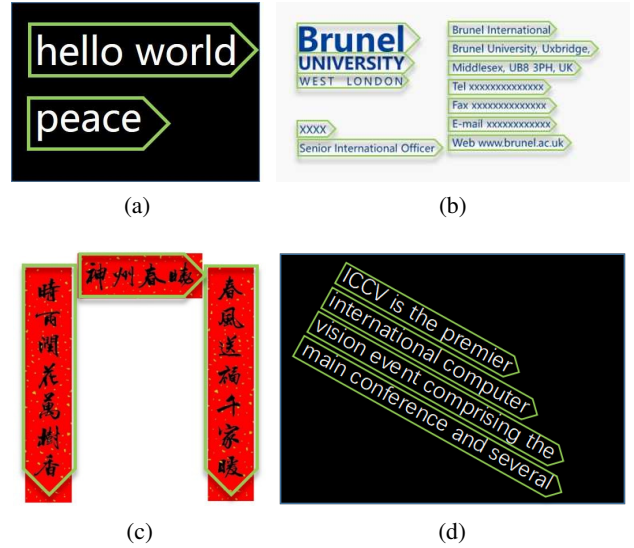


Figure 1: Examples of the MSR problem. (a)-(d) are 4 kinds of multi-sequence scenes. Each sequence is bounded by a green box with the arrow indicating text orientation.

well. Concretely, CTC can map a one-dimensional sequence of character probability distribution to a target sequence, but fails to map multi-dimensional probability distribution (*e.g.* the outputs of convolutional neural network) to multiple target sequences. Though *attention* can capture the attending area of each character from multi-dimensional feature maps to read multi-line text sequences (*e.g.* Fig. 1 (a)), it requires that the order of all lines constituting the sequence be pre-defined (as in [4]). In fact, it is usually impractical in some real cases (*e.g.* Fig. 1 (b) and (c)).

Therefore, we propose a novel **Multiple Sequence Recognition Approach** (*abbr.* MSRA) to simultaneously learn multiple text sequences from a multi-dimensional feature maps (*e.g.* the outputs of CNN or MDRNN [9]). Inspired by the concept of one-dimensional probability path in CTC, MSRA is responsible for selecting the optimal probability paths from a given two-dimensional probability space. And the path selection operation is the process of finding potential target sequences. Note that, MSRA is trained from the unordered set of multiple independent text sequences, which means that any ordered sequence-level annotations is acceptable during training. For example, annotations in Fig. 1(a) can be interpreted as {“helloworld”, “peace”} or {“peace”, “helloworld”}.

Major contributions of this paper are as follows:

1. Conceptually, we propose a new taxonomy of text recognition methods, i.e., NEE, QEE and PEE, and subsume the existing text sequence recognition works

into two types: single sequence recognition (SSR) and multiple sequence recognition (MSR). Then, we put forward a new and more challenging problem: recognizing multiple sequences from images by pure end-to-end learning, i.e., MSR by PEE.

2. We develop a novel PEE method MSRA to solve the MSR problem, in which the model is trained with only sequence-level text transcripts.
3. As we address a new problem, for evaluating the proposed method, we build up several datasets mainly based on the MNIST dataset and some real application scenarios including automatic bank card reading and ID card reading.
4. We conduct extensive experiments on these datasets, which show that the proposed method can effectively recognize multiple sequences from images, and outperforms two CTC/attention based baseline methods.

2. Related Work

Here, we review the major related works based on a new taxonomy of the existing solutions, which are subsumed to three types: NEE, QEE and PEE methods.

NEE. Wang *et al.* [33, 34] detected and recognized each character in an image with a sliding window, where the word is generated based on characters' global layout. However, the performance of such methods is limited due to poor representation of handcrafted features. After that, a number of approaches were proposed for solving the text localization task or the cropped text recognition task better.

For text localization, some recent methods [11, 14, 20, 22, 31, 37, 38] devoted to localizing entire text region with deep neural network techniques, instead of localizing characters one-by-one. These methods were trained with geometric annotations and greatly got better text region detection performance.

For text recognition, some early works designed complex handcrafted features such as connected components [26] or Hough voting [35] for character recognition, then integrated characters into words. Later, Jaderberg *et al.* [12] conducted a 90k-class classification task with a CNN, and generated words with a structured output layer, where each word corresponds to a class. But performance of such methods is impacted by the number of classes, and they cannot be extended to general character sequence generation. Recent works tended to treat the characters generation process as a sequence learning problem. Some CTC-based [28, 32] and attention-based [2, 6, 7, 16, 29, 30] methods were proposed for generating character sequence from a cropped text image, which were trained with text transcripts and achieved a big stride forward in performance.

Recently, Liao *et al.* [18, 19] integrated a text region detector and a text recognizer for end-to-end spotting text.

QEE. The success of deep learning in computer vision inspires a technical wave of reading text from images in an "end-to-end" way. Pioneering works in this direction [10, 17, 21] spotted text from images by first pre-training the detection module or recognition module, and then conducting a jointly training on the detection and recognition tasks. Then, Lyu *et al.* [23] proposed an end-to-end trainable text spotter by employing the character-level geometric annotations. Such methods still need both text transcripts and geometric annotations to train the model, so they are called *quasi-end-to-end* (QEE) methods.

PEE. Very recently, Bluche *et al.* [4] proposed a method to read multi-line text with a well-designed attention model, in which the order of all text lines constituting the sequence must be pre-defined. So what they handled is actually a SSR problem, only the text sequence may be split to several lines with predefined order and similar orientation.

In this paper, we address a new and more challenging problem: recognizing multiple text sequences from an image with only text (but no location) annotations. Here, the text sequences in the image are independent, they may have different text orientations, and no spatial order constraint exists among them. We propose a PEE method MSRA to solve this problem. Inspired by the idea of HMM-RNN hybrid [3, 5], MSRA directly maps the multi-dimensional outputs of network to all possible target sequences.

3. The MSRA Method

Here, we present the MSRA method in detail, including the problem formulation, algorithms, loss function and the training of MSRA as well as prediction using MSRA.

3.1. Formulation

MSRA aims to transform a multi-dimensional distribution $\mathbf{X} \in \mathbb{R}^{H \times W \times Q}$ (e.g. the forward results of CNN or MDRNN) as a conditional probability distribution over multiple character sequences, where Q , H and W are the number of character classes, the height and width of feature maps, respectively. Formally, \mathbf{X} is represented as

$$\mathbf{X} = \begin{pmatrix} x^{00} & x^{01} & \dots & x^{0W'} \\ x^{10} & x^{11} & \dots & x^{1W'} \\ \vdots & \vdots & \ddots & \vdots \\ x^{H'0} & x^{H'1} & \dots & x^{H'W'} \end{pmatrix}, \quad (1)$$

where $H'=H-1$ and $W'=W-1$, and $x^{i,j} \in \mathbb{R}^Q$ means the probability distribution at location (i, j) .

A character sequence is defined as a sequence of characters $\mathbf{l} \in (\Sigma^*)^*$, $|\mathbf{l}| > 0$, in which Σ^* is the set of all characters and an extra symbol *blank* representing character interval or non-text area. Then, the target $\mathbf{Z} = \{\mathbf{l}_1, \mathbf{l}_2, \dots, \mathbf{l}_N\}$ is

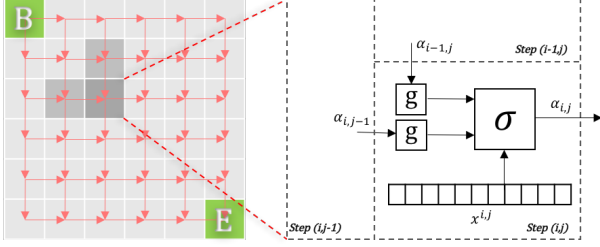


Figure 2: The illustration of path generation on the two-dimensional probability distribution \mathbf{X} . B and E separately denote the beginning position and ending position of path searching. For a cell (i, j) in \mathbf{X} , its state value $\alpha_{i,j}$ depends on both $\alpha_{i,j-1}$ and $\alpha_{i-1,j}$.

denoted as a set of multiple text sequences. Hereby, MSRA is devoted to maximizing the conditional probability

$$p(\mathbf{Z}|\mathbf{X}) \stackrel{def}{=} \frac{1}{N} \sum_{i=1}^N p(\mathbf{l}_i|\mathbf{X}), \quad (2)$$

where N is the number of sequences in \mathbf{Z} . Because of the independence between any two different character sequences, the calculation of $p(\mathbf{Z}|\mathbf{X})$ is equivalent to maximizing the conditional probability $p(\mathbf{l}|\mathbf{X})$ of each sequence over the input \mathbf{X} . Algorithms for evaluating $p(\mathbf{l}|\mathbf{X})$ are presented in the following subsection.

3.2. Algorithms

$p(\mathbf{l}|\mathbf{X})$ is the mapping condition probability of $\mathbf{l} \in \mathbf{Z}$ over the learnt two-dimensional probability distribution \mathbf{X} . By extending the concept of one-dimensional probability path in CTC, the evaluation of $p(\mathbf{l}|\mathbf{X})$ turns to solve the three-dimensional probability path $\bar{\mathbf{l}}$ search problem over \mathbf{X} , where $\bar{\mathbf{l}}$ is a path (as shown in Fig. 2) from the beginning $x^{0,0}$ to the end $x^{H',W'}$. $\bar{\mathbf{l}}$ is then mapped to a label sequence \mathbf{l} by using the *many-to-one* \mathcal{B} -mapping strategy in CTC [8]. Therefore, $p(\mathbf{l}|\mathbf{X})$ can be further rewritten as

$$p(\mathbf{l}|\mathbf{X}) = \sum_{\bar{\mathbf{l}} \in \mathcal{B}^{-1}(\mathbf{l})} p(\bar{\mathbf{l}}|\mathbf{X}). \quad (3)$$

In Eq. (3), $p(\bar{\mathbf{l}}|\mathbf{X})$ is further transferred as the prefix sub-path search problem, which can be iteratively calculated with a dynamic programming algorithm, as shown in the *Forward Algorithm*.

For representing the non-text areas, we also adopt: 1) the label sequence extension strategy, that is, adding blanks to the beginning and the end, and inserting blanks between each pair of neighboring characters, to get an extended sequence \mathbf{l}' ; and 2) the state transfer strategy, i.e., allowing

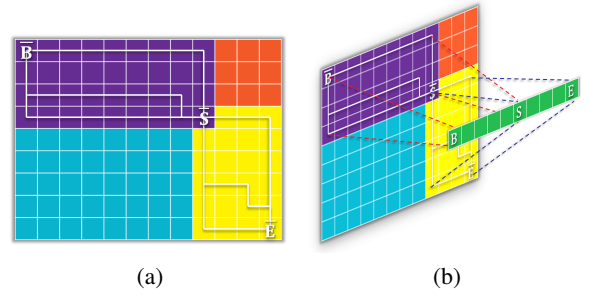


Figure 3: The illustration of the forward and backward algorithms matching the s position of \mathbf{l}' at $\bar{S}(i, j)$. In subgraph (a), the dark purple area represents the path search area of the forward algorithm, where the white paths $\bar{\mathbf{l}}$ from \bar{B} to \bar{S} are all solutions satisfying $\mathcal{B}(\bar{\mathbf{l}}) = \mathbf{l}'_{0:s}$. The yellow area represents the path search area of the backward algorithm, where the white paths $\bar{\mathbf{l}}$ from \bar{S} to \bar{E} are all solutions satisfying $\mathcal{B}(\bar{\mathbf{l}}) = \mathbf{l}'_{s:|\mathbf{l}'|-1}$. In subgraph (b), the green sequence represents \mathbf{l}' , in which B, S and E correspond to the location $0, s$ and $|\mathbf{l}'| - 1$, respectively. The forward calculation maps the paths from \bar{B} to \bar{S} in the deep purple area to the sequence from B to S , and the backward calculation maps the paths from \bar{S} to \bar{E} in the yellow area to the sequence from S to E .

path transitions between blank and any non-blank character, and any pair of distinct non-blank characters.

3.2.1 Forward Algorithm

We define $\alpha_{i,j}(s)$ as the probability for $\bar{\mathbf{l}}$ matching $\mathbf{l}'_{0:s}$ at (i, j)

$$\alpha_{i,j}(s) \stackrel{def}{=} \sum_{\bar{\mathbf{l}} \in \mathcal{B}^{-1}(\mathbf{l}'_{0:s})} \prod_{t=0}^{|\bar{\mathbf{l}}|-1} x_{\bar{\mathbf{l}}_t}^{i_t, j_t}, \quad (4)$$

where $\bar{\mathbf{l}}_t$ is the traversal of the path $\bar{\mathbf{l}}$, and i_t, j_t are the coordinates of the step that matches $\bar{\mathbf{l}}_t$. In Fig. 3(a), the white paths in the dark purple area (in the top-left corner) illustrate Eq. (4). Concretely, each of these white paths corresponds to an $\bar{\mathbf{l}}$ in Eq. (4).

The initialization rules of Eq. (4) are as follows:

$$\begin{aligned} \alpha_{0,0}(0) &= x_b^{0,0}, \\ \alpha_{0,0}(1) &= x_{l_1}^{0,0}, \\ \alpha_{0,0}(s) &= 0, \forall s > 2. \end{aligned} \quad (5)$$

$\alpha_{i,j}(s)$ can be iteratively calculated by

$$\begin{aligned} \alpha_{i,j}(s) &= \sigma(g(\alpha_{i,j-1}, s), g(\alpha_{i-1,j}, s)) \\ &= \lambda_1 g(\alpha_{i,j-1}, s) + \lambda_2 g(\alpha_{i-1,j}, s) \end{aligned} \quad (6)$$

where σ is a linear function for evaluating the path transitions from $(i-1, j)$ or $(i, j-1)$. λ_1, λ_2 are the hyper-parameters of σ . They will be detailed in the *Performance Evaluation* section.

And $g(\alpha_{i,j}, s)$ is denoted as

$$g(\alpha_{i,j}, s) \stackrel{def}{=} (\alpha_{i,j}(s) + \alpha_{i,j}(s-1) + \eta\alpha_{i,j}(s-2))x_{l'_s}^{i,j},$$

$$\eta = \begin{cases} 0 & \text{if } l'_s = \text{blank or } l'_s = l'_{s-2}, \\ 1 & \text{otherwise.} \end{cases} \quad (7)$$

In Eq. (6), there are two boundary problems to be considered:

1. $\alpha_{i,j}(s) = 0, \forall s < |l'| - 2(H-i+W-j-1)$ means that there are not enough locations to match the remaining characters in l' .
2. $\alpha_{i,j}(s) = 0, \forall s > 2(i+j)+1$ means that the matching position s is beyond the maximum length currently matchable.

At last, $p(l|\mathbf{X})$ is the sum of the prefix-path probabilities at (H', W') , i.e.,

$$p(l|\mathbf{X}) = \alpha_{H',W'}(|l'| - 1) + \alpha_{H',W'}(|l'| - 2). \quad (8)$$

3.2.2 Backward Algorithm

Similarly, we define $\beta_{i,j}(s)$ as the probability for \bar{l} matching $l'_{s:|l'|-1}$ at (i, j) but not relying on $x_{l'_0}^{i_0,j_0}$, that is,

$$\beta_{i,j}(s) \stackrel{def}{=} \sum_{\bar{l} \in \mathcal{B}(\bar{l})} \prod_{t=1}^{|\bar{l}|-1} x_{l'_t}^{i_t,j_t}, \quad (9)$$

where \bar{l}_t is the traversal of the path \bar{l} , and i_t, j_t are the coordinates of the step that matches \bar{l}_t . In Fig. 3(a), the white paths in the yellow area (in the bottom-right corner) illustrate Eq. (9). Concretely, each of these white paths corresponds to an \bar{l} in Eq. (9).

The initialisation rules for backward algorithm are as follows:

$$\begin{aligned} \beta_{H',W'}(|l'| - 1) &= 1, \\ \beta_{H',W'}(|l'| - 2) &= 1, \\ \beta_{H',W'}(s) &= 0, \forall s < |l'| - 2. \end{aligned} \quad (10)$$

Thus, $\beta_{i,j}(s)$ can be iteratively calculated as

$$\beta_{i,j}(s) = \lambda_1 g'(\beta_{i,j+1}, s) + \lambda_2 g'(\beta_{i+1,j}, s), \quad (11)$$

where

$$g'(\beta_{i,j}, s) \stackrel{def}{=} \beta_{i,j}(s)x_{l'_s}^{i,j} + \beta_{i,j}(s+1)x_{l'_{s+1}}^{i,j} + \eta'\beta_{i,j}(s+2)x_{l'_{s+2}}^{i,j},$$

$$\eta' = \begin{cases} 0 & \text{if } l'_s = \text{blank or } l'_s = l'_{s+2}, \\ 1 & \text{otherwise.} \end{cases} \quad (12)$$

The boundary considerations are the same as that in α computation.

3.3. Objective Function and Model Training

The objective function of MSRA is defined as the negative log probability of the correct complete-matching input set \mathcal{S} , that is

$$O = - \sum_{(\mathbf{X}, \mathbf{Z}) \in \mathcal{S}} \ln p(\mathbf{Z}|\mathbf{X}). \quad (13)$$

In order to train the model with the standard back-propagation algorithm [27], we need to derive the partial derivative of the objective function O with regards to $x_k^{i,j}$. By substituting Eq. (2) into Eq. (13), we can get

$$O = - \sum_{(\mathbf{X}, \mathbf{Z}) \in \mathcal{S}} (\ln \sum_{i=1}^N p(l_i|\mathbf{X}) - \ln N). \quad (14)$$

The gradient solving problem is transformed from a multi-sequence recognition problem to a single-sequence recognition problem. Then, we have

$$\frac{\partial p(l|\mathbf{X})}{\partial x_k^{i,j}} = \frac{1}{x_k^{i,j}} \sum_{s \in \text{lab}(l, k)} \alpha_{i,j}(s) \beta_{i,j}(s) \quad (15)$$

where $\text{lab}(l, k) = \{s : l'_s = k\}$. Finally, based on Eq. (14) and Eq. (15), we have

$$\frac{\partial O}{\partial x_k^{i,j}} = - \frac{1}{x_k^{i,j} \sum_{t=1}^n p(l_t|\mathbf{X})} \sum_{t=1}^n \sum_{s \in \text{lab}(l_t, k)} \alpha_{i,j}(s) \beta_{i,j}(s). \quad (16)$$

3.4. Prediction

The prediction process of MSRA is to generate multiple text sequences \mathbf{Z} from the learnt two-dimensional probability distribution \mathbf{X} . In our case, it is impractical to adopt the prefix search strategy used in CTC due to the following reasons:

- Since each step has two choices, prefix search will result in $O(2^N K)$ computational complexity, where K is the computational complexity of the prefix search method in CTC.

| Method | MS-MNIST[1] | | | MS-MNIST[2] | | | MS-MNIST[3] | | | MS-MNIST[4] | | | MS-MNIST[5] | | |
|------------------------|-------------|-------|-------|-------------|-------|-------|-------------|-------|-------|-------------|-------|-------|-------------|-------|-------|
| | NED | SA | IA | NED | SA | IA | NED | SA | IA | NED | SA | IA | NED | SA | IA |
| MSRA | 0.65 | 91.23 | 91.23 | 0.48 | 93.57 | 87.47 | 0.74 | 90.19 | 73.23 | 1.21 | 86.35 | 63.20 | 1.82 | 77.69 | 27.93 |
| Attention based method | 0.90 | 89.03 | 89.03 | 0.67 | 91.48 | 83.87 | 1.25 | 87.52 | 67.27 | 1.35 | 88.55 | 61.80 | 88.69 | 0 | 0 |
| CTC based method | 0.78 | 89.60 | 89.60 | - | - | - | - | - | - | - | - | - | - | - | - |

Table 3: Recognition results on MS-MNIST datasets. Only when all sequences in an image are recognized accurately, the image is considered being recognized accurately.

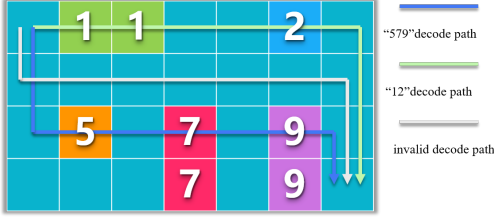


Figure 4: The illustration of the learnt maximum probability matrix of \mathbf{X} . Numbers in cells indicate the labels of predicted character classes, and blank cells have no character. The green path and blue path correspond to targets “12” and “579” respectively, while the gray path has only blanks.

- It is highly possible that paths contain only blanks (e.g. the gray path in Fig. 4), which makes prefix search to fail.

Even so, the prediction of MSRA can be solved in a task-specific way. That is, we can design the corresponding mapping strategies based on the specific scenarios. Given the learnt \mathbf{X} , we define the mapping function F to map the maximum probability matrix $M = \text{argmax}(\mathbf{X})$ to the target \mathbf{Z} by

$$\mathbf{Z} = F(\text{argmax}(\mathbf{X})). \quad (17)$$

Specifically, the function $F(\cdot)$ is formulated as

$$F(M) \stackrel{\text{def}}{=} \{\mathcal{B}(T_{r_{1,1}} + T_{r_{1,2}} + \dots); \mathcal{B}(T_{r_{2,1}} + T_{r_{2,2}} + \dots); \dots\}, \quad (18)$$

where

$$T_{r_{i,j}} \stackrel{\text{def}}{=} M_{r_{i,j}}[st_{r_{i,j}}, en_{r_{i,j}}] = \sum_{k=st_{r_{i,j}}}^{en_{r_{i,j}}} M_{r_{i,j},k} \quad (19)$$

where $r_{i,j}$ represents the row coordinate of the j -th string that is a substring of the i -th sequence to be generated from \mathbf{Z} . $M_{r_{i,j},k}$ is the value at $(r_{i,j}, k)$ in M . Then, F can be approximately learnt with a subset M' of M and the corresponding subset \mathbf{Z}' of \mathbf{Z} . The loss function is defined as

$$\mathcal{L} = \frac{1}{N} \sum_{i=1}^N \min_j NED(\mathbf{l}_i, \mathcal{B}(T_{r_{j,1}} + T_{r_{j,2}} + \dots)) \quad (20)$$

where NED is the edit distance normalized by the number of characters in \mathbf{l}_i , and N is the number of sequences contained in the samples of \mathbf{Z}' .

4. Performance Evaluation

In this section, we first evaluate the effectiveness of MSRA by comparing it with two CTC-based and attention-based baseline methods on multiple-sequence datasets generated based on MNIST [15], and visualize multiple sequences generation (the maximum probability paths) in α space. Then, we evaluate our method on four other datasets generated mainly based on two real application scenarios, including automatic bank card reading and ID card reading.

Note that this work addresses a new and very challenging problem, we evaluate our method on several synthetic datasets, and compare it with two CTC and attention based baseline methods. As an innovative and exploring work, we humbly believe that the current evaluation is enough to validate the effectiveness of the proposed method. We intend to leave further evaluation on popular datasets and comparison with other existing methods for a future work.



Figure 5: An example of multiple-sequence samples based on MNIST.

4.1. Performance on MNIST based Datasets

4.1.1 Datasets

We create MNIST-based multiple-sequence datasets by randomly selecting some digits from MNIST, and connecting them into a sequence. We superimpose no more than 5 such sequences into an image. Concretely, the process is like this: 1) each digit taken from MNIST has a size of 28×28 pixels, a horizontal-offset of ± 3 pixels, and a rotation angle of ± 10 ; 2) The number of sequences in images follows normal distribution approximately; 3) Each sequence

consists of no more than 14 above-mentioned digits, and sequence length obeys normal distribution approximately; 4) Sequences are superimposed to each image from top to bottom. Correspondingly, if the number of sequences in an image is k , the size of the image is $28k \times 392$. In addition, we add some noise data to each image. The noise data are digits randomly taken from MNIST with size of 7×7 pixels. The number of noise digits is one fifth of the valid digits contained in the image. Noise digits are superimposed to randomly selected positions in each image.

In such a way, we create five datasets, which are denoted by MS-MNIST[n] where n means that each image in the dataset contains at most n sequences, and $n=1, 2, 3, 4$ and 5 . We generate 27,000 samples for training and 3,000 samples for testing for each dataset.

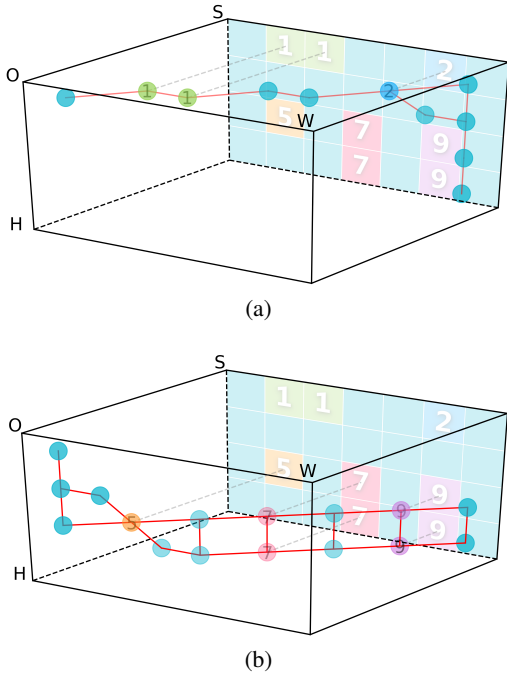


Figure 6: The illustration of decoding sequences (a) “12” and (b) “579”. $O \rightarrow W$, $O \rightarrow H$ and $O \rightarrow S$ mean the width dimension, the height dimension and the length to be matched, respectively. Each filled circle means the corresponding class at $\alpha_{i,j}(s)$.

4.1.2 Implementation details

Our method is implemented under the framework of Caffe [13]. We use 7 layers convolution structure (as in [28]) as the main network to extract image features, whose $\{\text{kernel size, channels, stride, pad}\}$ are $\{3, 64, 1, 1\}$, $\{3, 128, 1, 1\}$, $\{3, 128, 1, 1\}$, $\{3, 256, 1, 1\}$, $\{3, 256, 1, 1\}$, $\{3, 512, 1, 1\}$ and $\{3, 512, 1, 1\}$, respectively.

Each convolution layer follows a Relu [25] activation layer. There is a pool layer after the 1st, 2nd, 4th, 6th convolution layers, its kernel size is 2×2 . Then, three methods, 2 CTC/attention based baseline methods and our MSRA, are used to process the features, respectively.

MSRA and the CTC based method compute their respective constructed losses with the output of the softmax layer. While the attention based method is implemented roughly (but not completely) as in [4]. Note that in our attention based method, it is necessary to re-calibrate the corresponding unordered sequence set from top to bottom and add a *line break symbol* class between the sequences.

All networks are trained with the ADADELTA [36] optimization method, and λ_1, λ_2 are set to 0.9, 0.1. Our experiments are performed on a workstation with an Intel Xeon(R) E5-2650 2.30GHz CPU, an NVIDIA Tesla P40 GPU and 128GB RAM.

4.1.3 Results

Tab. 3 shows the recognition results of the three methods mentioned above. NED(%) is normalized edit distance [24], SA(%) is sequence recognition accuracy, and IA(%) is image recognition accuracy. As we can see from the table, our MSRA method achieves better performance in all cases than the other two methods, and the CTC based method is unable to identify multiple text sequences in an image. Though the attention based method shows acceptable performance when the number of sequences contained in images is small, but its performance degrades rapidly when the number of sequences contained in images increases to 5.

More importantly, MSRA can be trained with unordered sequence calibration, while the attention based method requires the text sequences in training images to be calibrated from top to bottom, which actually reveals the sequences’ spatial layout information. When the attention based method uses disordered sequence calibration, the model can not converge. That is, it can not identify the situation. As ordered calibration is a subset of disordered calibration, using ordered calibration in MSRA does not affect the results.

We also visualize the matching paths for decoding text sequences in α space. Fig. 6 presents the visualization of prefix path matching probability α in an image containing two sequences “12” and “579”. Concretely, Fig. 6(a) and (b) separately show the matching process of the extended sequences “-1-2-” and “-5-7-9-” in α space. Here, ‘-’ denotes the blank class. In each sub-figure, the corresponding maximum probability matrix of conditional probability distribution is given on the back side of the cuboid. The projection of each path along the $O \rightarrow S$ dimension is consistent with the result of the maximum probability class map. Note that there are multiple paths for each target sequence. For



Figure 7: Samples of four more challenging datasets: (a) IDN, (b) BCN, (c) HV-MNIST, and (d) SET.

example, Fig. 6(b), there are 2 and 6 possible paths before and after the ‘5’ position, which results in totally 12 possible matching paths.

4.2. Performance on More Challenging Datasets

In this part, we set up four more challenging datasets mainly based on real application scenarios, and train the MSRA model to recognize text sequences from images in these datasets, which are described in detail as follows:

- **Identification card number dataset (IDN).** We create the IDN dataset by considering the standard font size and type used in the standard ID card. Here, we just recognize the digital information in ID cards, including the ID card number, birthdate of the ID holder etc.
- **Bank card number dataset (BCN).** We generate the BCN according to the standard font size and type commonly used in 161 major banks. We also just recognize the digital information including bank card number and valid period.
- **Horizontal and vertical MNIST dataset (HV-MNIST).** In this dataset, a horizontal sequence and a vertical sequence appear in each image. Each sequence consists of 5 handwritten digits from MNIST and some noise just like in MS-MNIST datasets.
- **Synthetic English Text dataset (SET).** We use 70 character-classes (26 capitals, 26 lowercase letters, 10 numbers and 8 other characters such as ‘,’ ‘.’ ‘:’ ‘(’ ‘)’, ‘[’ ‘]’ ‘ ’) to generate multi-line English text based on some English documents downloaded from Web. The font is *Times New Roman*. We randomly select a document and then randomly select a part of it as the label to generate image data.

Fig. 7 shows some samples of the four datasets above, each of which contains 27,000 samples for training and 3,000 samples for testing.

For the four datasets, the network structure used in experiments is similar to that used for the MS-MNIST

datasets. The difference lies in the number and location of the pool layer and the reshape parameters of the input layer. Because we must ensure that \mathbf{X} has the ability to hold multiple text sequences, in both horizontal and vertical directions. For example, in the HV-MNIST dataset, we control the size of \mathbf{X} to 14×14 for covering the extended length (11) of label strings, and some additional space to ensure that beginning step and the end step are blank.

| Datasets | NED | SA | IA |
|----------|------|-------|-------|
| IDN | 0.59 | 97.59 | 90.39 |
| BCN | 0.12 | 98.12 | 96.23 |
| HV-MNIST | 1.87 | 90.99 | 82.73 |
| SET | 1.48 | 68.57 | 47.90 |

Table 4: Recognition results on datasets IDN, BCN, HV-MNIST and SET. NED, IA and SA are all evaluated in terms of percentage.

Tab. 4 shows the recognition results of our method on the four datasets. We can see that our method still achieves promising performance. MSRA performs satisfactorily on IDN and BCN though data in these datasets are based on real applications. Results on HV-MNIST demonstrate that MSRA can handle complex MSR problems where an image has text sequences of different orientations. Our method has the lowest performance on SET, because data in SET are more complex in terms of the number of classes and the length of sequences. The increase of class number means that for each step the method faces more matching options. While the increase of sequence length means that a larger \mathbf{X} is required to accommodate sequence information. Though these datasets have more noise caused by complex background, different orientations, font size and type etc., MSRA still performs well.

5. Conclusion

In this paper, we address a novel and challenging problem, recognizing multiple text sequences from images by pure end-to-end learning. To this end, we propose an effective approach called MSRA. Different from the existing methods, MSRA directly trains and identifies multiple text sequences in a pure end-to-end way without using any geometric annotations. Experiments on several multiple text sequences datasets show that our MSRA method is effective and achieves better performance than two CTC and attention based baseline methods. In the future, on the one hand, we will conduct more comprehensive performance evaluation on the MSRA method with public datasets; On the other hand, we will explore more advanced pure end-to-end techniques to solve the MSR problem.

References

- [1] D. Bahdanau, K. Cho, and Y. Bengio. Neural Machine Translation by Jointly Learning to Align and Translate. In *ICLR*, 2015. 2
- [2] F. Bai, Z. Cheng, Y. Niu, S. Pu, and S. Zhou. Edit Probability for Scene Text Recognition. In *CVPR*, pages 1508–1516, 2018. 3
- [3] Y. Bengio. Markovian Models for Sequential Data. *Neural Computing Surveys*, 2(199):129–162, 1999. 3
- [4] T. Bluche, J. Louradour, and R. Messina. Scan, Attend and Read: End-to-End Handwritten Paragraph Recognition with MDLSTM Attention. In *ICDAR*, volume 1, pages 1050–1055, 2017. 1, 2, 3, 7
- [5] H. A. Bourlard and N. Morgan. *CONNECTIONIST SPEECH RECOGNITION: A Hybrid Approach*, volume 247. Springer Science & Business Media, 2012. 3
- [6] Z. Cheng, F. Bai, Y. Xu, G. Zheng, S. Pu, and S. Zhou. Focusing Attention: Towards Accurate Text Recognition in Natural Images. In *ICCV*, pages 5086–5094, 2017. 1, 3
- [7] Z. Cheng, Y. Xu, F. Bai, Y. Niu, S. Pu, and S. Zhou. AON: Towards Arbitrarily-Oriented Text Recognition. In *CVPR*, pages 5571–5579, 2018. 3
- [8] A. Graves, S. Fernández, F. Gomez, and J. Schmidhuber. Connectionist Temporal Classification: Labelling Unsegmented Sequence Data with Recurrent Neural Networks. In *ICML*, pages 369–376, 2006. 2, 4
- [9] A. Graves and J. Schmidhuber. Offline Handwriting Recognition with Multidimensional Recurrent Neural Networks. In *NIPS*, pages 545–552, 2009. 2
- [10] T. He, Z. Tian, W. Huang, C. Shen, Y. Qiao, and C. Sun. An End-to-End TextSpotter With Explicit Alignment and Attention. In *CVPR*, pages 5020–5029, 2018. 1, 2, 3
- [11] H. Hu, C. Zhang, Y. Luo, Y. Wang, J. Han, and E. Ding. WordSup: Exploiting Word Annotations for Character Based Text Detection. In *ICCV*, pages 4940–4949, 2017. 3
- [12] M. Jaderberg, K. Simonyan, A. Vedaldi, and A. Zisserman. Reading Text in the Wild with Convolutional Neural Networks. *IJCV*, 116(1):1–20, 2016. 1, 3
- [13] Jia, Yangqing, Shelhamer, Evan, Donahue, Jeff, Karayev, Sergey, Long, and Jonathan. Caffe: Convolutional Architecture for Fast Feature Embedding. In *ACM MM*, pages 675–678, 2014. 7
- [14] Y. Jiang, X. Zhu, X. Wang, S. Yang, W. Li, H. Wang, P. Fu, and Z. Luo. R2CNN: Rotational Region CNN for Orientation Robust Scene Text Detection. *CoRR*, abs/1706.09579, 2017. 3
- [15] Y. LeCun, L. Bottou, Y. Bengio, and P. Haffner. Gradient-Based Learning Applied to Document Recognition. *Proceedings of the IEEE*, 86(11):2278–2324, 1998. 6
- [16] C.-Y. Lee and S. Osindero. Recursive Recurrent Nets with Attention Modeling for OCR in the Wild. In *CVPR*, pages 2231–2239, 2016. 3
- [17] H. Li, P. Wang, and C. Shen. Towards End-to-end Text Spotting with Convolutional Recurrent Neural Networks. In *ICCV*, pages 5238–5246, 2017. 1, 2, 3
- [18] M. Liao, B. Shi, and X. Bai. Textboxes++: A single-shot oriented scene text detector. *IEEE TIP*, 27(8):3676–3690, 2018. 1, 2, 3
- [19] M. Liao, B. Shi, X. Bai, X. Wang, and W. Liu. TextBoxes: A Fast Text Detector with a Single Deep Neural Network. In *AAAI*, pages 4161–4167, 2017. 1, 2, 3
- [20] M. Liao, Z. Zhu, B. Shi, G.-s. Xia, and X. Bai. Rotation-Sensitive Regression for Oriented Scene Text Detection. In *CVPR*, pages 5909–5918, 2018. 3
- [21] X. Liu, D. Liang, S. Yan, D. Chen, Y. Qiao, and J. Yan. FOTS: Fast Oriented Text Spotting with a Unified Network. In *CVPR*, pages 5676–5685, 2018. 1, 2, 3
- [22] Y. Liu and L. Jin. Deep Matching Prior Network: Toward Tighter Multi-oriented Text Detection. In *CVPR*, pages 3454–3461, 2017. 3
- [23] P. Lyu, M. Liao, C. Yao, W. Wu, and X. Bai. Mask textspotter: An end-to-end trainable neural network for spotting text with arbitrary shapes. In *ECCV*, pages 67–83, 2018. 2, 3
- [24] A. Marzal and E. Vidal. Computation of Normalized Edit Distance and Applications. *IEEE TPAMI*, 15(9):926–932, 1993. 7
- [25] V. Nair and G. E. Hinton. Rectified Linear Units Improve Restricted Boltzmann Machines. In *ICML*, pages 807–814, 2010. 7
- [26] L. Neumann and J. Matas. Real-Time Scene Text Localization and Recognition. In *CVPR*, pages 3538–3545, 2012. 3
- [27] D. E. Rumelhart, G. E. Hinton, and R. J. Williams. Learning representations by back-propagating errors. *Nature*, 323(6088):533, 1986. 5
- [28] B. Shi, X. Bai, and C. Yao. An End-to-End Trainable Neural Network for Image-based Sequence Recognition and Its Application to Scene Text Recognition. *IEEE TPAMI*, 39(11):2298–2304, 2017. 1, 3, 7
- [29] B. Shi, X. Wang, P. Lyu, C. Yao, and X. Bai. Robust Scene Text Recognition with Automatic Rectification. In *CVPR*, pages 4168–4176, 2016. 3
- [30] B. Shi, M. Yang, X. Wang, P. Lyu, C. Yao, and X. Bai. Aster: An Attentional Scene Text Recognizer with Flexible Rectification. *IEEE TPAMI*, pages 1–1, 2018. 1, 3

- [31] F. Wang, L. Zhao, X. Li, X. Wang, and D. Tao. Geometry-Aware Scene Text Detection With Instance Transformation Network. In *CVPR*, pages 1381–1389, 2018. 3
- [32] J. Wang and X. Hu. Gated Recurrent Convolution Neural Network for OCR. In *NIPS*, pages 335–344, 2017. 3
- [33] K. Wang, B. Babenko, and S. Belongie. End-to-End Scene Text Recognition. In *ICCV*, pages 1457–1464, 2011. 1, 2, 3
- [34] K. Wang and S. Belongie. Word Spotting in the wild. In *ECCV*, pages 591–604. Springer, 2010. 1, 2, 3
- [35] C. Yao, X. Bai, B. Shi, and W. Liu. Strokelets: A Learned Multi-scale Representation for Scene Text Recognition. In *CVPR*, pages 4042–4049, 2014. 3
- [36] M. D. Zeiler. ADADELTA: AN ADAPTIVE LEARNING RATE METHOD. *arXiv preprint arXiv:1212.5701*, 2012. 7
- [37] Z. Zhong, L. Sun, and Q. Huo. An Anchor-Free Region Proposal Network for Faster R-CNN based Text Detection Approaches. *CoRR*, abs/1804.09003, 2018. 3
- [38] X. Zhou, C. Yao, H. Wen, Y. Wang, S. Zhou, W. He, and J. Liang. EAST: An Efficient and Accurate Scene Text Detector. In *CVPR*, pages 5551–5560, 2017. 3